Clim. Past Discuss., https://doi.org/10.5194/cp-2018-164
Manuscript under review for journal Clim. Past
Discussion started: 10 December 2018

Climate of the Past Discussions

Identifying teleconnections and multidecadal variability of East Asian surface temperature during the last millennium in CMIP5 simulations

Satyaban B. Ratna[1], Timothy J. Osborn[1], Manoj Joshi[1], Bao Yang[2], Jianglin Wang[2]

[1]Climatic Research Unit, School of Environmental Sciences, University of East Anglia, Norwich, NR2 2BP, United Kingdom
[2]Key Laboratory of Desert and Desertification, Northwest Institute of Eco-Environment and Resources, Chinese Academy of Sciences, Lanzhou, 730000, China

Correspondence to: Satyaban B. Ratna (s.bishoyi-ratna@uea.ac.uk)

Abstract. We examine the relationships in models and reconstructions between the multidecadal variability of surface temperature in East Asia and two extratropical modes of variability: the Atlantic Multidecadal Oscillation (AMO) and the Pacific Decadal oscillation (PDO). We analyze the spatial, temporal and spectral characteristics of the climate modes in Last Millennium, Historical and pre-industrial control simulations of three CMIP5/PMIP3 GCMs, to assess the relative influences of external forcing and unforced variability. These models produce PDO and AMO variability with realistic spatial patterns and their spectral characteristics. AMO internal variability strongly influences East Asia temperature in one model (bcc-csm1-1), but has a weak influence in the other two (CCSM4 and MPI-ESM-P). In all three models, external forcing greatly strengthens these statistical associations and hence the apparent teleconnection with the AMO. PDO internal variability strongly influences East Asian temperature in two of the three models, but external forcing makes this apparent teleconnection much weaker. This indicates that the AMO-East Asian temperature relationship is partly driven by external forcing whereas the PDO-temperature relationship is largely driven by internal variability. External forcing confounds attempts to diagnose the teleconnections of internal multidecadal variability. Using AMO and PDO indices that represent internal variability more closely and minimising the influence of external forcing on East Asia temperature can partly ameliorate this confounding effect. Nevertheless, these approaches still yield differences between the forced and control simulations and they cannot always be applied to paleoclimate reconstructions, so we recommend caution when interpreting internal variability teleconnections diagnosed from reconstructions that contain both forced and internal variations.

1 Introduction

Coupled ocean-atmosphere processes cause climate variations on interannual to multidecadal timescales (Dai et al., 2015 and Steinman et al., 2015), resulting in persistent temperature and hydroclimate anomalies over both adjacent continents and remote regions (Wang et al. 2017; Coats and Smerdon, 2017), potentially having both immediate and long lasting consequences for society (Büntgen et al., 2011). Assessing teleconnections between ocean and land can be done using a number of methods, each of which have their limitations. The usefulness of the observational record for understanding multidecadal teleconnections is limited by its length. Paleoclimate reconstructions can provide information on longer time scales, and can also place the

Clim. Past Discuss., https://doi.org/10.5194/cp-2018-164
Manuscript under review for journal Clim. Past
Discussion started: 10 December 2018

current climate regime in a long-term perspective. Several reconstructions of modes of climatic variability such as the Atlantic Multidecadal Oscillation (AMO) and the Pacific Decadal Oscillation (PDO) have been attempted using networks of proxy data, including tree-ring, ice cores, speleothems, coral growth, lake sediments, and documentary evidence (e.g. MacDonald and Case, 2005, Mann et al, 2009, Wang et al, 2017, Fang et al. 2018b, Wang et al. 2018). However, limitations in the geographic and temporal coverage of the proxy records, including terrestrial and marine locations, and differing climatic and seasonal sensitivities, affect the ability of these reconstructions to fully represent decadal to centennial variability (Jones et al, 2009; Christiansen and Ljungqvist, 2017).

Global climate model (GCM) simulations can offer complementary long-term perspectives on the behaviour of important modes of climate variability (Atwood et al, 2016; Fleming and Anchukaitis, 2016; Landrum et al, 2013). Such models can also be used to identify the extent of large scale teleconnections between these modes and regional climate (Coats et al., 2013). GCMs also provide a means of separating changes associated with external forcing from those arising by internal variability since they can be run using differing boundary conditions (Schurer et al., 2013, 2014). Atmosphere-ocean coupled GCMs with more extensive representation of processes within the climate system components also permit more detailed examination of spatial and temporal variations during the last millennium.

The focus of our study is on the annual mean temperature of East Asia on multidecadal and longer timescales. On these timescales, variability associated with the AMO (Schlesinger and Ramankutty, 1994; Kerr, 2000; Delworth and Mann, 2000) and PDO (Mantua et al. 1997; Newman et al., 2016) can exert an important influence on the climate over Asia (Qian et al. 2014; Wang et al. 2013; Dong 2016; Li et al. 2017; Fang et al. 2018a). Our aims are to: (1) identify the key teleconnections between the AMO, PDO and East Asian temperature in climate models; (2) to determine how external forcings affect these simulated teleconnections; (3) contrast the simulated and reconstructed behaviour of East Asian temperatures on multidecadal timescales; (4) develop recommendations for making unbiased comparisons between model data and paleoclimate reconstructions. We also provide insight into the long-term simulated behaviour of these modes of climate variability with respect to the external forcing and internal variability.

The rest of the article is organised as follows: Section 2 describes the climate models and paleoclimate data used in this study, and the methods to calculate the climate indices. Section 3 describes the results associated with AMO and its teleconnection with East Asian surface temperature and Section 4 discusses the results associated with the relationship between PDO and East Asian surface temperature. The role of volcanic forcing on these aspects of climate variability is demonstrated in Section 5. In Section 6, further results are discussed and conclusions are summarised.

Clim. Past Discuss., https://doi.org/10.5194/cp-2018-164
Manuscript under review for journal Clim. Past
Discussion started: 10 December 2018

2 Data and Methods

2.1 Climate model simulations

We select models from the Coupled Model Intercomparison Project Phase 5 (CMIP5; Taylor et al. 2012) that had provided output for all three experiments considered here: (i) pre-industrial control (PC) run with constant external forcing, (ii) Last Millennium (LM) and (iii) Historical experiments (HIST) with external forcings. Of the six GCMs that met this criterion, three models (MIROC, FGOALS, GISS) were excluded because they show a strong drift in the last millennium or control simulations (Artwood et al. 2016, Fleming and Anchukaitis, 2016; Bothe et al., 2013). Details of the remaining three GCMs are summarised in Table 1. The forcing and boundary conditions for the LM simulations follow the protocols of Paleoclimate Model Intercomparison Project Phase 3 (PMIP3) as discussed by Schmidt et al. (2012). The forcings are composed of volcanic aerosols, solar radiation, greenhouse gas (CH_4, CO_2, and N_2O) concentrations, and anthropogenic land-use changes over the period 850-1849. The HIST simulations are forced with natural and anthropogenic forcing over the period 1850-2005.The comparison of these 'forced' simulations with 'unforced' control simulations provide a means of assessing what portion of the variability is attributed to external forcing and what portion reflects purely internal variability. Also, these simulations are useful in providing longer term perspective for detection and attribution studies.

We interpolate output from the BCC and MPI models to the CCSM4 grid resolution to facilitate intercomparison. We note that the available model simulations were not necessarily continuous from their LM simulations into their HIST simulations, so modes of variability cannot be calculated across 1850. Each model version was same across the all simulations. Since our focus is on natural variability arising from internal and external causes, we have minimised the influence of any residual long-term drift or of anthropogenic transient forcings in the GCM simulations by first detrending (removing the linear trend) across the Last Millennium (850-1849) and historical (1850-2000) time series separately and then merging them into a continuous detrended timeseries for the period 850-2000 (LMH hereafter).

2.2 Diagnosing Atlantic and Pacific variability

The AMO index is calculated from the area-weighted North Atlantic (80W – 0W, 0-65N) monthly mean SST anomaly for the LMH and PC simulations. When the value of the index is positive (negative), it is known as the warm (cold) phase of the AMO. We have considered here two sets of AMO indices, both with (hereafter, AMOrem) and without (hereafter, AMOnorem) first subtracting the global mean SST anomaly time series (Trenberth and Shea, 2006) from the spatially averaged (North Atlantic) time series anomalies at each time interval. Atlantic SST will exhibit both internal variability and the response to external forcings: by subtracting the global-mean SST anomaly, the AMOrem index will reflect more closely the variability that is focussed on the North Atlantic region and not the signal of external forcing present in the global SST pattern. The AMO

indices generated by the above two methods are regressed over the North Atlantic SSTs (Fig 1) which shows the spatial pattern of the AMO.

The PDO index is calculated as the leading mode from an empirical orthogonal function (EOF) analysis of monthly residual SST anomalies in the north Pacific region 20-65°N and 110°E-110°W, which are calculated by first removing the long-term monthly means and then subtracting the monthly mean global SST anomaly at each time interval. The EOF analysis yields spatial patterns (loadings) and temporal scores (time series). In its warm/positive (cool/negative) phase, SSTs are above (below) normal along the west coast of North America and below (above) average in the central north Pacific (Fig. 2).We don't see much differences in the EOF loading among the three models but there is considerable differences in their time series.

The model simulated AMO and PDO indices are generated using monthly mean SSTs for the LMH (850–2000) and PC simulations, and then converted into annual mean values for our analysis. For temperature over East Asia (TAS), we also consider warm (April-September) and cold (October-March) season averages.

2.3 Paleoclimate and volcanic forcing reconstructions

The BCC and CCSM4 GCMs used volcanic forcing from Gao et al. (2008, hereafter GRA) and MPI used volcanic forcing from Crowley et al. (2008, hereafter CEA) in their last millennium simulations (Table 1). Accordingly, we compare the model and reconstructed data with GRA and CEA, as well as a volcanic forcing reconstruction from Sigl et al. 2015 (hereafter, SIG).

We used proxy-based reconstructions for the AMO, PDO and surface temperature over East Asia (TAS) as summarised in Table 2. Two AMO reconstructions are used in this study. Mann et al (2009) reconstructed near-global fields of surface temperature using a diverse mix of annual and decadal resolution tree-ring, coral, ice core and sediments records from across the globe. Their AMO series (hereafter AMN09) was computed from the North Atlantic SST grid cells of their reconstructed fields and extends for the period 500-2006 with 10-year low-pass filters. The annually resolved AMO by Wang et al (2017) is based on tree ring, ice core, historical records only from circum-Atlantic land regions and is available for the period 800-2010. Wang et al. (2017) first reconstruct Atlantic Multidecadal Variability (hereafter WN17V) and then subtract an estimate of the externally-forced component to obtain a series that represents mostly internal variability, denoted the Atlantic Multidecadal Oscillation (hereafter WN17O). The two AMO reconstructions (AMN09 and WN17V) provide estimates of the full (both external and internal) variability of the North Atlantic SST. Although Mann et al. (2009) reconstructed near-global SST fields, we have not subtracted the global-mean SST from the Atlantic-mean SST to isolate the *internal* AMO variability (cf. the 'AMOrem' series from the models) because prior to 1600 their reconstruction is a linear combination of only two spatial patterns which gives limited information about the Atlantic–global SST difference. Wang et al (2017) did attempt to isolate the internal variability by regressing against solar and volcanic forcing reconstructions, to yield the WN17O series also considered here.

Clim. Past Discuss., https://doi.org/10.5194/cp-2018-164
Manuscript under review for journal Clim. Past
Discussion started: 10 December 2018

One annual mean PDO reconstruction is based on Mann et al (2009) as described above and hereafter denoted as PMN09. This series is an average of SST grid cells over the central north Pacific region (22.5^0N–57.5^0N, 152.5^0E–132.5^0W): since this region has mostly negative loadings in our EOF-based PDO index (Fig 2), we multiply PMN09 by minus one to make it comparable to the other PDO indices. Another annually resolved PDO index is from MacDonald and Case (2005; hereafter, MD05) who used only tree ring records from *Pinus flexilis* in California and Alberta to reconstruct PDO for the period 993-1996. The PDO reconstructions, unlike the EOF-based definition in modeled and observed SST dataset, might also contain some signal of external forcing because the proxy records, used in reconstructions, largely suffer from influence of external forcing.

The East Asian temperature reconstruction for the warm season is from Wang et al. (2018, hereafter WN18), which uses the mean of seven published reconstructions and is available for the period 850-1999. See Wang et al. (2018) for a discussion of the underlying reconstructions and their similarity/differences.

It should be noted that the time sequences of the reconstructed and simulated data are not directly comparable because each will have its own realisation of internal variability. They should, however, be internally consistent so that their teleconnections can be compared on multidecadal time scales, along with any contribution that is externally forced (to the extent that the external forcing matches between the datasets).

2.4 Analysis methods

Since our focus is to understand climate variability on multidecadal timescales, all the time series are passed through a 30-year low pass filter using the Lanczos filter. The correlation analyses are tested for statistical significance using the two-tailed student's t-test. The number of degrees of freedom are the number of 30-year long segments minus 2, i.e if low pass filtered 1000-year long time series has 33 independent samples (1000/30) and 31 degrees of freedom. The corresponding critical correlation value is used to test the statistical significance at 90% or 95% level. The null hypothesis (that the correlation is zero) is rejected if the correlation value is greater than the critical correlation value.

Spectral analysis to identify the spectral shape and any major periodicities of AMO and PDO is performed via the Fast Fourier Transform (FFT). The statistical significance of the spectra was tested against a red noise background (Mann and Lees, 1996) and the periodicities at multidecadal time scales that are significant at 90% level are emphasized. In order to isolate the near-internal variability from the LMH model runs, we regress out the influence of volcanic forcing from the TAS, AMO and PDO timeseries by calculating the regression coefficient of the GRA or CEA volcanic global forcing timeseries against the TAS, AMO and PDO time series, respectively.

Clim. Past Discuss., https://doi.org/10.5194/cp-2018-164
Manuscript under review for journal Clim. Past
Discussion started: 10 December 2018

3. Influences of Atlantic Multidecadal Oscillation

Figure 3 shows the correlation between the AMO index and multidecadal variations in surface temperature in the LMH and PC simulations. The correlation with *area-averaged* East Asia surface temperature (TAS) is also calculated (Fig. 4). In the PC simulations with no external radiative forcing, internal climate variability alone results in correlations between the AMO and East Asian temperature that are generally positive (Fig. 3a, b, c), though only the MPI model shows widespread statistically significance on a point-by-point basis (Fig. 4) – i.e. a warmer North Atlantic Ocean is associated with warmer East Asian temperatures. The strength of the correlation is very sensitive to the presence of external forcing, becoming more strongly positive both spatially (Fig. 3g, h, i) and area-averaged basis (Fig. 4) in the LMH run (i.e. increasing from 0.32, 0.29 and 0.71 for the BCC, CCSM4 and MPI PC runs respectively, to 0.62, 0.85 and 0.84 in the LMH run). For all the three models, the strong positive correlation occurs mostly because natural external (e.g., volcanic eruptions) forcings cause concurrent warming or cooling in both the Atlantic and East Asian regions (Fig. 7).

When we remove the global SST anomaly before calculating the AMO index, its association with TAS becomes much weaker, especially for LMH runs, as shown in Fig. 3 (j, k, l vs g, h, i), and Fig. 4 AMOrem vs AMOnorem. This is because much of the external forcing influence on N Atlantic SST also drives global SST, so subtraction of the global-mean SST anomaly prior to the calculation of the AMO removes this externally-forced variability from the AMO. However, because TAS has a different sensitivity to global forcings such as volcanic eruptions, the correlation is decreased, rather than falling to insignificant values. For the MPI model, there is a clear association between the AMO and East Asian temperatures that is generated by internal variability, especially in the northern half of the region considered here, since a positive correlation occurs even in the PC run (Fig. 3c and f). This remains even if the global SST anomaly is subtracted, suggesting that this mode of internal variability only partly projects onto global-mean SST anomalies. If the AMOrem index is used, then the correlation is weaker in the LMH run than in the PC run for the MPI model. This is because the forcings generate a response in the TAS but not in the AMO (any response is mostly removed because global SST is subtracted from Atlantic SST), weakening their correlation. This behaviour is not seen in the other two models because the AMOrem index has little correlation with TAS even in their unforced PC runs.

These dependencies of the model correlations on the presence of external forcing and on the calculation of the AMO index are important in the context of interpreting reconstructed data. Suppose we wish to use reconstructed data to answer the question "does the AMO, as a mode of *internal* variability, influence E Asian temperatures on multidecadal timescales?" The reconstructions represent the real world (a situation with external forcings) and some AMO reconstructions (e.g. AMN09 and WN17V) have not isolated internal variability of the N Atlantic SST from externally-forced signals (because, for instance, global-mean SST cannot be subtracted before calculating the AMO if global SST has not been independently reconstructed). This situation is equivalent to of Fig. 3g, h, i (LMH runs with AMOnorem indices) and a strong positive correlation might be

Clim. Past Discuss., https://doi.org/10.5194/cp-2018-164
Manuscript under review for journal Clim. Past
Discussion started: 10 December 2018

found between the AMO and E Asian temperatures – but this would *not* establish that the AMO, as a mode of internal climate variability, was strongly influencing E Asian temperatures on multidecadal timescales.

The WN18 E Asian reconstruction represents *warm-season* temperature, so we repeated our model analysis but using both warm and cold season temperatures and obtained results that are closely consistent with those using annual-mean temperatures. The reconstructed AMO series all show positive correlations with the WN18 E Asian temperature reconstruction (Fig. 4). Those representing full AMO variability (WN17V and AMN09) have correlations around 0.4, while the correlation with E Asian temperature falls towards 0.24 (which is not significant) for the WN17O series representing only internal AMO variability.

None of the reconstructed AMO or E Asian surface temperature series correlate significantly with the equivalent simulated series from the LMH runs, indicating that internal variability and any errors in reconstructed climate and forcings dominate the influence of external forcing, or that model response to forcings is unrealistic.

4. Influences of Pacific Decadal Oscillation

Similar to the AMO analysis, Figs 5 and 6 show the correlation between PDO and TAS. The PDO is mostly negatively correlated with TAS except for a small region in southern parts of India and Southeast Asia in all the three models, with the correlation being strongest in the north east of the region (Fig. 5). This is expected because cooler SSTs lie adjacent to this region when the PDO index is positive (Fig. 2). The correlation between the PDO and TAS is therefore negative, though varying widely in strength between the models especially for the PC runs (see Fig. 6). These correlations weaken when external forcing is applied to the models (except for the MPI model where it was already weak), suggesting that external forcing drives additional variability in East Asian temperatures but not in the PDO (because we subtract the global-mean SST anomaly prior to calculating it, and use an EOF definition that depends on SST spatial differences rather than mean SST across the North Pacific, Fig. 2). Using this definition (rather than a simple area-mean SST), the model PDOs do not have strong or consistent responses to forcing in the LMH simulations, in agreement with Landrum et al. (2013) and Fleming and Anchukaitis (2016).

We have also compared the reconstructed PDO and TAS time series (Fig. 6). The correlations are also negative: MD05-WN18 and PMN09-WN18 are -0.10 and -0.41, respectively, and only the latter is significant. The weak correlation with MD05 might be partly related to the fact that this reconstruction is based on only two tree-ring records of North America, suggesting a possible uncertainty if teleconnection patterns it relied on change through time. The simulated PDO series show very weak correlations with the reconstructed PDO series: as with the AMO, this implies that an external forcing influence is weak compared with internal variability and reconstruction errors, or that models' PDO response to forcings is unrealistic. For the simulated PDO indices, any external forcing influence may be weak if the PDO calculation (an EOF analysis with the global-

Clim. Past Discuss., https://doi.org/10.5194/cp-2018-164
Manuscript under review for journal Clim. Past
Discussion started: 10 December 2018

mean SST removed) effectively removes a forcing signal. As before, we repeated our model analysis using both warm and cold season E Asian temperatures and found very similar results to the annual temperatures.

5. Effect of volcanic forcing

The behaviour of the AMO and PDO timeseries and their correlation with E Asian temperature are clearly sensitive to the presence of external forcing (e.g. LMH versus PC differences), so we now consider the effect of volcanic forcing- the largest external influence within the Last Millennium runs (Atwood et al. 2016). Previous studies indicated that the Little Ice Age and other cooling periods during the last millennium are largely driven by volcanic forcing (Briffa et al. 1998; Ammann et al. 2007; Atwood et al. 2016). All the three volcanic forcing timeseries (GRA, CEA and SIG) are closely correlated with each other but are by no means identical (Fig. 7a). For the period A.D. 850-2000, their correlations are 0.75 (GRA and CEA), 0.81 (GRA and SIG) and 0.82 (CEA and SIG), highlighting the value in considering multiple forcing histories.

The timeseries for CCSM4 and MPI display a strong association between volcanic forcing and model simulated TAS and AMO (Fig. 7), confirmed by the correlations (Fig. 8). These models simulate a significantly colder climate over East Asia in response to volcanic forcing compared to BCC, which is especially evident during the three periods containing strong eruptions (1257/8, 1458/9 and 1815). The case is same for the AMOnorem time series, with the models simulating cold Atlantic SST anomalies during the periods of strong volcanic eruptions, with high correlations for CCSM4 and MPI ranging from 0.49 to 0.73 with all the three volcanic forcing datasets. Similarly, the correlation between volcanic forcing and TAS are high (0.58 to 0.79) for the CCSM4 and MPI. These strong positive correlations demonstrate that natural external forcings largely cause concurrent warming or cooling in both the Atlantic and East Asian regions, contributing to the positive correlations found earlier between AMOnorem and TAS in these models (Fig. 3g, h, i). Removing the global SST anomaly first to obtain the AMOrem index renders the correlations with volcanic forcing insignificant (Fig. 8) and the AMOrem time series (Fig. 7d) do not show any cooling with corresponding volcanic forcing eruptions. This contributes to the much-reduced correlations with TAS when the AMOrem series are used (Fig. 4).

The TAS-volcanic forcing relationship in the BCC model is notably weaker as is the AMO-volcanic forcing relationship (Fig. 8). This behaviour is the same if we use warm or cold-season TAS (not shown) rather than annual-mean TAS. The smaller influence of volcanic forcing for BCC partly explains why it has a weaker correlation between TAS and AMOnorem compared to the CCSM4 and MPI models during the LMH simulations. The very weak BCC response to volcanic eruptions compared to CCSM4 and MPI models can be understood by comparing effective volcanic forcings in the three GCMs. To do this, we analyse net incoming shortwave radiation anomalies composited for the three largest volcanic eruption events (1257, 1458 and 1815) in all three models. Fig 9 shows that the decrease in the net incoming shortwave radiation following these eruptions in BCC is only ~20% of the response in both CCSM4 and MPI.

Clim. Past Discuss., https://doi.org/10.5194/cp-2018-164
Manuscript under review for journal Clim. Past
Discussion started: 10 December 2018

Since we can diagnose AMO and PDO timeseries that are not significantly correlated with volcanic forcing (Fig. 8: AMOrem and the EOF-based PDO), we further tried factoring out the volcanic influence from the TAS time series to see if we could reproduce the behaviour of the control runs (PC) if we only had data from the forced runs (LMH). This is akin to trying to identify the behaviour of internal variability in the real Earth system (Steinman et al., 2015; Dai et al., 2015). We regressed volcanic forcing (GRA for BCC and CCSM4, and CEA for MPI here) on the TAS data, and removed it to yield a TAS series without the linear influence of the volcanic forcing (See section 2.4 for detail). Factoring out volcanic forcing from TAS did weaken the correlations with the simulated AMO LMH series (Fig. 4; AMOrem vs AMOrem_vo) especially for CCSM4 and MPI. For example, the correlations (Fig. 4) between AMOnorem and TAS fall from 0.62–0.85 (AMOnorem) to 0.44–0.59 (AMOnorem_vo) and from 0.12-0.36 (AMOrem) to 0.12-0.23 (AMOrem_vo). The correlation didn't weak much for BCC (Fig. 4; AMOrem vs AMOrem_vo) because it simulates only a weak volcanic influence on E Asian temperature. Despite factoring out the influence of the dominant forcing and using a definition (AMOrem) that yields an AMO index that is not strongly correlated with forcing, we still find very different behaviour in the PC simulation than in the LMH simulation for the MPI model: in the former, the role of AMO internal variability on E Asian temperature especially for the south part of E Asia is comparatively small than the latter. For the other two models, we can correctly infer the small role of AMO internal variability from the LMH run provided we factor out the influence of external forcings.

In terms of Pacific variability, the PDO is not strongly correlated with volcanic forcing: correlations are near zero for the BCC and CCSM4 models and slightly negative for MPI (Fig. 7e; Fig. 8). However, the CCSM4 and MPI models simulate strong positive correlations between East Asian TAS and volcanic forcing. This additional externally-forced variability in East Asian temperatures (due to the direct radiative cooling following strong volcanic eruptions) weakens the negative PDO-TAS correlation for BCC and CCSM4 (Fig. 6) but slightly strengthens it for MPI (likely because of the negative PDO-volcanic correlation). Factoring out the volcanic signal from TAS hardly changes the relationship between E Asian TAS and the PDO (LMH_vo; Fig. 6). This indicates that for two models (BCC and CCSM4), we are not able to determine the internal variability teleconnection between PDO and TAS when external forcings are present even by using a PDO definition that is insensitive to external forcing and by factoring out the volcanic influence on TAS.

These results indicate that the surface temperature multidecadal variability over East Asia is strongly modulated by the external forcing rather than internal variability in two of the models (Fig. 8). The percentages of variance (r^2) explained by the volcanic forcing are 62 % and 59 % for CCSM4 and MPI, respectively. This is in contrast to the WN18 TAS reconstruction, which shows no significant correlation with the volcanic series (WN18 also report that the volcanic signal is small compared with other influences). The PDO reconstructions show weakly negative (PMN09) or near-zero (MD05) correlations with volcanic forcing, similar to the models. The AMO reconstructions by AMN09 and WN17V show positive correlation with the volcanic forcing time series, similar to the BCC model but much weaker than the other two models for the equivalent AMO index definitions (AMOnorem).

Clim. Past Discuss., https://doi.org/10.5194/cp-2018-164
Manuscript under review for journal Clim. Past
Discussion started: 10 December 2018

To further assess the role of external forcing, the power spectra of the AMO and PDO indices are analysed (Fig.10 and 11, respectively) for the PC and LMH experiments. All models display red spectra with pronounced multidecadal variability but they differ in their peak frequencies. For the AMOnorem method of diagnosing the AMO index, the inclusion of external forcing (LMH runs) greatly strengthens the redness and multidecadal power of the variability for the CCSM4 and MPI models; the increase is more moderate for BCC. Removing the global-mean SST first (AMOrem), reduces the difference between the PC and LMH runs. The peak AMO frequency in BCC is about 20 years in most cases but there is a secondary peak around 60-80 years for AMOrem in the LMH run. CCSM4 shows significant AMOrem spectral peaks at ~40 years (both PC and LMH) and also at ~20 years in the LMH run. The MPI has the reddest AMO spectra in all cases, with some runs/definitions showing peak power at ~50 years. The AMO reconstructed spectra allows us a comparison (Fig. 10a) – not of the periodicity but of the overall spectral shape. CCSM4 and MPI models have the reddest spectra and for AMOnorem LMH these are qualitatively similar to the spectra of the WN17V and AMN09 reconstructions, while the BCC model shows much less multi-decadal power. In the case of the PDO, all three models show red spectra with enhanced power at ~15-20 years for both PC and LMH simulations, indicating that the Pacific variability arises mostly by internal variability. Landrum et al. (2013) found the same frequency for both control and last millennium simulations. The enhanced PDO power at ~15-20 years is filtered out by the 30-year smoothing used for the majority of analyses reported here, which might weaken the PDO-TAS correlation.

6. Discussion and Conclusions

The instrumental record is too short to clearly distinguish the contributions from natural internal variability, natural forcings and anthropogenic forcings at multidecadal timescales. Zhang et al. (2018) and Wang et al. (2018) have explored this issue using paleoclimate reconstructions of temperatures over a large region in E Asia. Here, we complement these studies by using the dynamical information provided by three climate models (Table 1), with and without the influence of external forcings over the last millennium. Our key findings are:

1. The models simulate multidecadal modes of variability in the extratropical oceans (AMO and PDO) with spatial patterns similar to those previously identified in the observations and proxy-based reconstructions. Using commonly applied methods to diagnose their time series (area-averaged N Atlantic SST for the AMO and the leading EOF of N Pacific SST for the PDO) we find that they have red spectra with enhanced multi-decadal variability similar to those found in observation and reconstructions. The shape of their spectra and the periods that have power significantly above the background spectrum differ between the models and with the presence or absence of external forcing.

2. These multidecadal modes of variability, along with variations in volcanic forcing, are found to influence E Asian temperature in the models. In most cases, E Asia temperature is positively correlated with the AMO and volcanic forcing, and negatively correlated with the PDO. The correlations are not spatially uniform, with PDO correlations

strongest in the parts of the E Asian region that are closest to the extratropical N Pacific Ocean, and the AMO influence showing some latitudinal differences.

3. The presence of external forcing strongly affects the apparent teleconnections between these multidecadal modes of variability and E Asia temperature. The effect depends on how the modes of variability are diagnosed and whether the forcings add common variability to both series or add distinct variance to E Asia temperature but not to the mode of variability.

4. If the AMO is defined simply as the mean N Atlantic SST then external forcing strengthens the AMO-E Asia temperature correlation by causing concurrent warming or cooling in both the Atlantic and E Asian regions. For all three models, the correlations between E Asian temperature and the AMO are stronger in the last millennium forced simulation than in their corresponding control runs when the AMO is defined this way.

5. Defining the AMO as the difference between N Atlantic and global-mean SST reduces but does not completely remove this effect, because much but not all of the external forcing influence on N Atlantic SST also drives global SST in these models. The AMO-E Asian temperature correlation is then much weaker in these models, and regressing out the influence of the dominant forcing (volcanic) from E Asian temperature further modifies this correlation.

6. The PDO definition used here (the leading EOF of Pacific SST minus global-mean SST) yields an index that has only weak correlations with volcanic forcing. Despite this, the multidecadal correlation between the PDO and E Asia temperature (which is negative) is still sensitive to the presence of external forcing. In this case, external forcing weakens the apparent teleconnection in two of the models. This partly arises because external forcing (especially volcanic forcing) generates a response in E Asia temperature but not in the PDO index, thus weakening the correlation between them. Regressing out the influence of volcanic forcing on E Asia temperature has relatively limited effect on the correlation, which remains much weaker than in the control run for two of the models.

These results have significant implications for attempts to determine the influence of the AMO and the PDO strictly as modes of *internal* variability on E Asia temperatures. With models, we can simply analyse their control runs. For the real world, we do not have that option: we can analyse only reconstructions from a real world in which natural external forcings are present. In this case, we recommend, on the basis of our results, that careful consideration be given to separating out the influence of external forcings on both the indices of modes of variability and on the E Asia temperature series before determining the internal variability teleconnections.

There are a number of ways to attempt this, each with its own limitations. The modes of variability might be defined using the difference between regional and global SST, however in many cases a separate reconstruction of global SST may not be available. Mann et al. (2009) reconstructed a global field of SST but prior to 1600 their reconstruction is a linear combination

of only two spatial patterns which gives limited information about the Atlantic–global SST difference. Another approach is to identify and remove the influence of external forcing, e.g. by regression against forcing histories in reconstructions (Wang et al., 2017, 2018), by a method combining observations with ensemble of coupled climate model simulations (Dai et al., 2015 and Steinman et al., 2015),or using more sophisticated detection and attribution methods (e.g. Hegerl and Zwiers, 2011). These approaches require accurate forcing histories. A further approach is to use an EOF-based definition of the index where the spatial pattern has regions with loadings of opposite sign. External forcing tends to project similarly onto regions with opposite signs, cancelling out much of its influence on the resulting index. This is appropriate for the PDO, as used here, but less so for the AMO because the associated SST pattern is dominated by anomalies of the same sign (Fig. 1). Regression against forcing histories can also be used to remove the influence of external forcing on the target region (E Asian temperature for this study), prior to identifying the influence of AMO and PDO variability (Wang et al., 2018).

Even if these approaches are taken, it may still be impossible to determine the influence of multidecadal internal variability by analysing data that has been subject to external forcings. Despite factoring out the influence of the volcanic forcing in the AMO index, we still find very different behaviour in the forced simulation than in the control run for the MPI model. In the forced run, the apparent AMO teleconnection on E Asian temperature is rather weak (AMOrem_vo in Fig. 4), whereas in the control run it is strong. For the other two models, we can correctly infer that the AMO internal variability has only a small influence on E Asia temperature from the forced run provided we factor out the influence of external forcings. Similar limitations were found regarding the PDO teleconnection: for two models (BCC and CCSM4), we are not able to determine its strongly negative correlation with E Asia temperature internal variability from a simulation with external forcings. We note the possibility that external forcing may have modified the dynamical behaviour of the internal variability in these cases, confounding the notion that we can clearly separate forced change from internal variability.

Finally, we found only partial agreement between the behaviours shown by the reconstructions and models. The correlations between E Asia temperature and the AMO and PDO showed the same signs in the models and the data, but the correlation values had a wide range. The strong influence of volcanic forcing in two of the models was not found in the reconstructions (Wang et al. 2018). We need to be careful while interpreting the results of the CMIP5-PMIP3 last millennium simulations in light of the paleoclimate record, because there exists a large uncertainties in the characterization of volcanic forcing, reconstruction of aerosol loading, optical depth and aerosol effective radius as a function of time, latitude, and height in the atmosphere, all of which exert important controls on the climate system (Atwood et al. 2016).

Acknowledgements.

Support provided by the Belmont Forum and JPI-Climate project INTEGRATE (An Integrated data-model study of interactions between tropical monsoons and extratropical climate variability and extremes) with funding by UK NERC grant

Clim. Past Discuss., https://doi.org/10.5194/cp-2018-164
Manuscript under review for journal Clim. Past
Discussion started: 10 December 2018

NE/P006809/1. J.W. also acknowledges the support by the National Key R&D Program of China (grant: 2017YFA0603302) and the National Science Foundation of China (NSFC; grant: 41602192).

References

Ammann, C. M., Joos, F., Schimel, D., Otto-Bliesner, B., and Tomas, R.: Solar influence on climate during the past millennium: Results from transient simulations with the NCAR Climate System Model, Proc. Natl. Acad. Sci., 104, 3713, doi:10.1073/pnas.0605064103, 2007.

Atwood, A. R., Wu, E., Frierson, D. M. W., Battisti, D. S., and Sachs, J. P.: Quantifying climate forcings and feedbacks over the last millennium in the CMIP5-PMIP3, J. Climate, 29, 1161– 1178, 2016.

Bothe, O., Jungclaus, J. H., and Zanchettin, D.: Consistency of the multi-model CMIP5/PMIP3-past1000 ensemble, Clim. Past, 9, 2471–2487, doi:10.5194/cp-9-2471-2013, 2013.

Briffa, K. R., Jones, P. D., Schweingruber, F. H., and Osborn, T. J.: Influence of volcanic eruptions on Northern Hemisphere summer temperature over the past 600 years. Nature, 393, 450–455, 1998.

Buntgen, U., Tegel, W., Nicolussi, K., McCormick, M., Frank, D., Trouet, V., Kaplan, J. O., Herzig, F., Heussner, K.-U., and Wanner, H.: 2500 years of European climate variability and human susceptibility, Science, 331, 578–582, 2011.

Christiansen, B., and Ljungqvist, F. C.: Challenges and perspectives for large-scale temperature reconstructions of the past two millennia. Reviews of Geophysics, 55, 40-96, 2017.

Coats, S., and Smerdon, J. E.: Climate variability: The Atlantic's internal drum beat. Nat. Geosci., 10, 470-471, 2017.

Coats, S., Smerdon, J. E., Cook, B. I., and Seager, R.: Stationarity of the tropical Pacific teleconnection to North America in CMIP5/PMIP3 model simulations. Geophys. Res. Lett., 40, 4927–4932, 2013.

Crowley, T. J., Zielinski, G., Vinther, B., Udisti, R., Kreutz, K., Cole-Dai, J., and Castellano, E.: Volcanism and the Little IceAge, PAGES Newslett., 16, 22–23, 2008.

Dai, A., Fyfe, J. C., Xie, S.-P., and Dai, X.: Decadal modulation of global surface temperature by internal climate variability. Nat. Clim. Change, 5, 555-559, 2015.

Delworth, T. L., and Mann, M. E.: Observed and simulated multidecadal variability in the Northern Hemisphere. Climate Dyn., 16, 661–676, 2000.

Fang, K., Cook, E., Guo, Z., Chen, D., Ou, T., Zhao, Y.: Syncronous multi-decadal climate variability of the whole Pacific areas revealed in tree rings since 1567.Environ. Res. Lett. 13 024016, 2018b.

Fang, K., Guo, Z., Chen, D., Wang, L., Dong, Z., Zhou, F., Zhao, Y., Li, J., Li, Y., Cao, X.: Interdecadal modulation of the Atlantic Multi-decadal Oscillation (AMO) on southwest China's temperature over the past 250 years. Clim Dyn., https://doi.org/10.1007/s00382-018-4244-x, 2018a.

Fleming, L. E., Anchukaitis, K. J.: North Pacific decadal variability in the CMIP5 last millennium simulations. Clim. Dyn., doi: 10.1007/s00382-016-3041-7, 2016.

Gao, C., Robock, A., and Ammann, C.: Volcanic forcing of climate over the past 1500 years: An improved ice core-based index for climate models. J. Geophys. Res., 113, D231111, doi:https://doi.org/10.1029/2008JD010239, 2008.

Giorgetta, M. A., Jungclaus, J., Reick, C. H., Legutke, S., Bader, J., Böttinger, M., Brovkin, V., Crueger, T., Esch, M., Fieg, K., Glushak, K., Gayler, V., Haak, H., Hollweg, H.-D., Ilyina, T., Kinne, S., Kornblueh, L., Matei, D., Mauritsen, T., Mikolajewicz, U., Mueller, W., Notz, D., Pithan, F., Raddatz, T., Rast, S., Redler, R., Roeckner, E., Schmidt, H., Schnur, R., Segschneider, J., Six, K. D., Stockhause, M., Timmreck, C., Wegner, J., Widmann, H., Wieners, K.-H., Claussen, M., Marotzke, J., and Stevens, B.: Climate and carbon cycle changes from 1850 to 2100 in MPI-ESM simulations for the coupled model intercomparison project phase 5, J. Adv. Model. Earth Syst., 5, 572–597, doi:10.1002/jame.20038, 2013.

Hegerl, G., and Zwiers, F.: Use of models in detection and attribution of climate change. Wiley Interdiscip. Rev.: Climate Change, 2, 570–591, 2011.

Jones, P. D., Briffa, K. R., Osborn, T. J., Lough, J. M., van Ommen, T. D., Vinther, B. M., Luterbacher, J., Wahl, E. R., Zwiers, F. W., Mann, M. E., Schmidt, G. A., Ammann, C. M., Buckley, B. M., Cobb, K. M., Esper, J., Goosse, H., Graham, N., Jansen, E., Kiefer, T., Kull, C., Kuttel, M., Mosley-Thompson, E., Overpeck, ¨ J. T., Riedwyl, N., Schulz, M., Tudhope, A. W., Villalba, R., Wanner, H., Wolff, E., and Xoplaki, E.: High-resolution palaeoclimatology of the last millennium: a review of current status and future prospects, The Holocene, 19, 3–49, 2009.

Kerr, R. A.: A North Atlantic climate pacemaker for the centuries. Science, 288, 1984-1985, 2000.

Landrum, L., Otto-Bliesner, B. L., Wahl, E. R., Conley, A., Lawrence, P. J., Rosenbloom, N., and Teng, H.: Last Millennium Climate and Its Variability in CCSM4, J. Climate, 26, 1085– 1111, doi:10.1175/JCLI-D-11-00326.1, 2013.

Li, X. et al. The East Asian summer monsoon variability over the last 145 years inferred from the Shihua Cave record, North China. Sci. Rep. 7, 7078, https://doi.org/10.1038/s41598-017-07251-3 (2017).

Li, X. L., Cheng, H., Tan, L. C., Ban, F. M., Sinha, A., Duan, W. H., Li, H. Y., Zhang, H. W., Ning, Y. F., Kathtayat, G., Edwards, R. L.: The East Asian summer monsoon variability over the last 145 years inferred from the Shihua Cave record, North China. Sci Rep 7:7078, 2017.

MacDonald, G. M., and Case, R. A.: Variations in the Pacific decadal oscillation over the past millennium. Geophys. Res. Lett., 32, L08703, doi:10.1029/2005GL022478, 2005.

Mann, M. E., Zhang, Z., Rutherford, S., Bradley, R. S., Hughes, M. K., Shindell, D., Ammann, C., Faluvegi, G., and Ni, F.: Global signatures and dynamical origins of the Little Ice Age and Medieval Climate Anomaly, Science, 326, 1256–1260, 2009.

Mann, M. E., and Lees, J. M.: Robust estimation of background noise and signal detection in climatic time series. Clim. Change, 33, 409-445, 1996.

Mantua, N. J., Hare, S. R., Zhang, Y., Wallace, J. M. and Francis, R. C.: A Pacific interdecadal climate oscillation with impacts on salmon production. Bull. Amer. Meteor. Soc., 78, 1069–1079, 1997.

Newman, M., and Coauthors, 2016: The Pacific Decadal Oscillation, Revisited. J. Clim., 29, 4399-4427.

Newman, M., Alexander, M. A., Ault, T. R., Cobb, K. M., Deser, C., Di Lorenzo, E., Mantua, N. J., Miller, A. J., Minobe, S., Nakamura, H., Schneider, N.: The Pacific decadal oscillation, revisited. J Clim. Doi: 10.1175/JCLI-D-15-0508.1, 2016.

Qian, C. C., Yu, J.-Y., and Chen, G.: Decadal summer drought frequency in China: the increasing influence of the Atlantic Multi-decadal Oscillation. Environmental Research Letters, 9, 124004, 2014.

Schlesinger, M. E., and Ramankutty, N.: An oscillation in the global climate system of period 65–70 years. Nature, 367, 723–726., 1994.

Schmidt, G. A., Jungclaus, J. H., Ammann, C. M., Bard, E., Braconnot, P., Crowley, T. J., Delaygue, G., Joos, F., Krivova, N. A., Muscheler, R., Otto-Bliesner, B. L., Pongratz, J., Shindell, D. T., Solanki, S. K., Steinhilber, F., and Vieira, L. E. A.: Climate forcing reconstructions for use in PMIP simulations of the Last Millennium (v1.1), Geosci. Model Dev., 5, 185–191, doi:10.5194/gmd-5-185-2012, 2012.

Schurer, A. P., Hegerl, G. C., Mann, M. E., Tett, S. F. B., and Phipps, S. J.: Separating forced from chaotic climate variability over the past millennium. J. Clim., 26, 6954-6973, 2013.

Schurer, A. P., Tett, S. F. B., and Hegerl, G. C.: Small influence of solar variability on climate over the past millennium. Nat. Geosci., 7, 104-108, 2014.

Sigl, M., Winstrup, M., McConnell, J. R., Welten, K. C., Plunkett, G., Ludlow, F., Buntgen, U., Caffee, M., Chellman, N., Dahl-Jensen, D., Fischer, H., Kipfstuhl, S., Kostick, C., Maselli, O. J., Mekhaldi, F., Mulvaney, R., Muscheler, R., Pasteris, D. R., Pilcher, J. R., Salzer, M., Schupbach, S., Steffensen, J. P., Vinther, B. M., and Woodruff, T. E.: Timing and climate forcing of volcanic eruptions for the past 2,500 years, Nature, 523, 543–549, doi:10.1038/nature14565, 2015.

Steinman, B. A., Mann, M. E., and Miller, S. K.: Atlantic and Pacific multidecadal oscillations and Northern Hemisphere temperatures. Science, 347, 988-991, 2015.

Taylor, K. E., Stouffer, R. J. and Meehl, G. A.: An overview of CMIP5 and the experiment design. Bull. Amer. Meteor. Soc., 93, 485–498, doi:https://doi.org/10.1175/BAMS-D-11-00094.1, 2012.

Trenberth, K. E., and Shea, D. J.: Atlantic hurricanes and natural variability in 2005. Geophys. Res. Lett., 33.L12704, doi:10.1029/2006GL026894, 2006.

Wang, J., Yang, B., Osborn, T. J., Ljungqvist, F. C., Zhang, H., and Luterbacher, J.: Causes of East Asiantemperature multidecadal variability during the last millennium. Geop. Res. Lett, Revised, 2018.

Wang, J., Yang, B., Ljungqvist, F. C., and Zhao, Y.: The relationship between the Atlantic Multidecadal Oscillation and temperature variability in China during the last millennium. J. Quat. Sci., 28, 653–658, doi:https://doi.org/10.1002/jqs.2658, 2013.

Wang, J., Yang, B., Ljungqvist, F. C., Luterbacher, J., Osborn, T. J., Briffa, K. R., and Zorita, E.: Internal and external forcing of multidecadal Atlantic climate variability over the past 1,200 years. Nat. Geosci, 10, 512–517, doi:https://doi.org/10.1038/ngeo2962, 2017.

Xin, X. G., Wu, T. W., Li, J. L., Zhi, W. Z., Li, W. P., Wu, F. H.: How well does BCC CSM1.1 reproduce the 20th century climate change over China? Atmos Ocean Sci Lett., 6, 21–26, 2013.

Zhang, H., Werner, J. P. García-Bustamante, E., González-Rouco, F., Wagner, S., Zorita, E., Fraedrich, K., Ljungqvist, F. C., Zhu, X., Xoplaki, E., Chen, F., Duan, J., Ge, Q., Hao, Z., Ivanov, M., Schneider, L., Talento, S., Wang, J., Yang, B., and Luterbacher, J.: East Asian warm season temperature variations over the past two millennia, Scientific Reports, *8*, 7702, 2018.

Clim. Past Discuss., https://doi.org/10.5194/cp-2018-164
Manuscript under review for journal Clim. Past
Discussion started: 10 December 2018

Climate of the Past Discussions

Table 1: Summary of the CMIP5-PMIP3 climate models considered in this study and the volcanic forcing applied in their Last Millennium simulations. The simulation length of last millennium and Historical simulations together for all the three models are 1151 years (850-2000). The simulation length in the Pre-industrial control run for BCC, CCSM4 and MPI are 500 years, 1050 and 1150 years respectively.

Model (abbr.)	**Institution**	**Reference**	**Atmospheric resolution**	**Ocean resolution**	**Volcanic forcing**
bcc-csm1-1 (BCC)	Beijing Climate Center	Xin et al. (2013)	128x64 L26	360x232 L40	Gao et al. (2008)
CCSM4 (CCSM4)	National Center for Atmospheric Research	Landrum et al. (2013)	288x192 L26	320x384 L60	Gao et al. (2008)
MPI-ESM-P (MPI)	Max Planck Institute for Meteorology	Giorgetta et al. (2013)	196x98 L47	256x220 L40	Crowley et al. (2008)

5

Clim. Past Discuss., https://doi.org/10.5194/cp-2018-164
Manuscript under review for journal Clim. Past
Discussion started: 10 December 2018

Table 2: Summary of the paleo reconstructions considered in this study

Reconstruction (abbr.)	Reference	Variable	Time span	Data source
AMO (AMN09)	Mann et al. (2009)	N Atlantic average SST	500-2006	Tree ring, coral, ice & sediment cores
AMO (WN17V and WN17O)	Wang et al. (2017)	N Atlantic(0-70°N) average SST	800-2010	Tree ring, ice core, documentary
PDO (PMN09)	Mann et al. (2009)	N Pacific (22.5-57.5°N, 152.5°E-132.5°W) average SST	500-2006	Tree ring, coral, ice& sediment cores
PDO (MD05)	MacDonald & Case (2005)	N Pacific (north of 20°N) principal component of SST	993-1996	Tree ring
TAS (WN18)	Wang et al. (2018)	E Asia land air temperature	850-1999	Mean of 7 available reconstructions

Clim. Past Discuss., https://doi.org/10.5194/cp-2018-164
Manuscript under review for journal Clim. Past
Discussion started: 10 December 2018

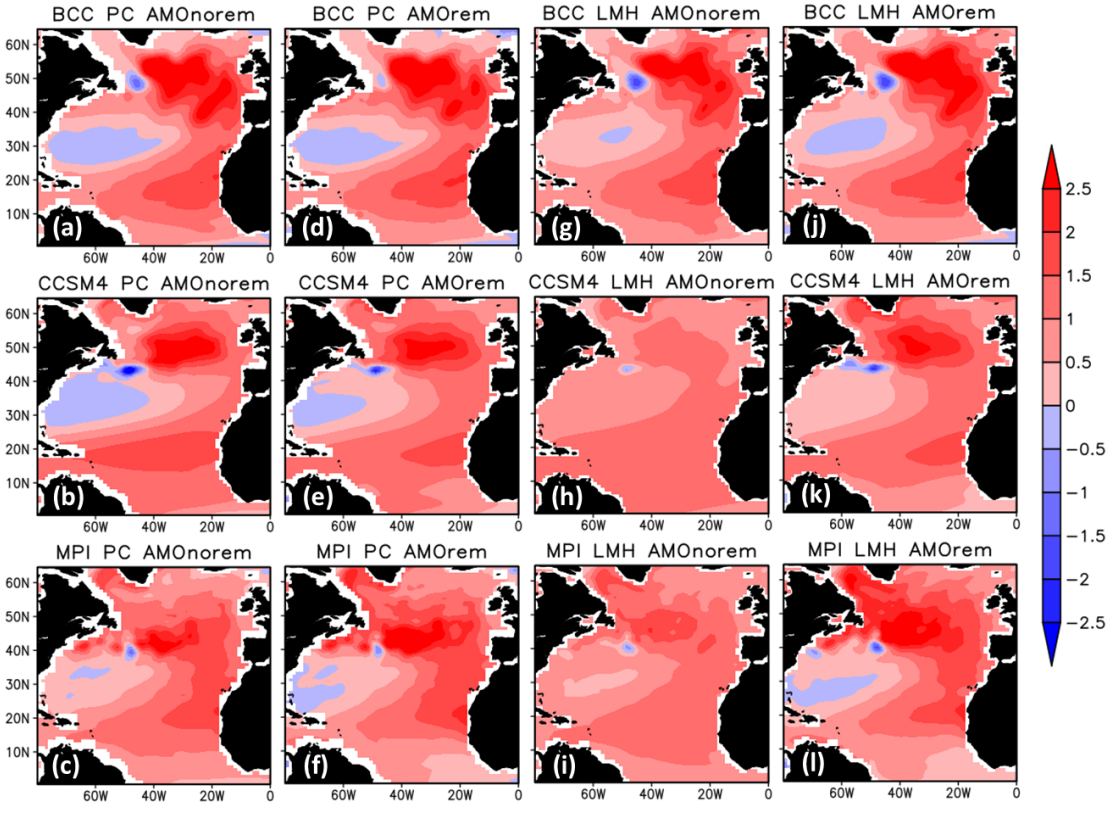

Figure 1: The AMO spatial patterns. Regression of annual-mean SST (K) on the AMO index for the three CMIP models for the LMH and PC experiments. (a, b, c) and (g, h, i) use the AMO index calculated without subtracting the global SST anomaly while (d, e, f) and (j, k, l) use the AMO index after subtracting the global SST anomaly.

Clim. Past Discuss., https://doi.org/10.5194/cp-2018-164
Manuscript under review for journal Clim. Past
Discussion started: 10 December 2018

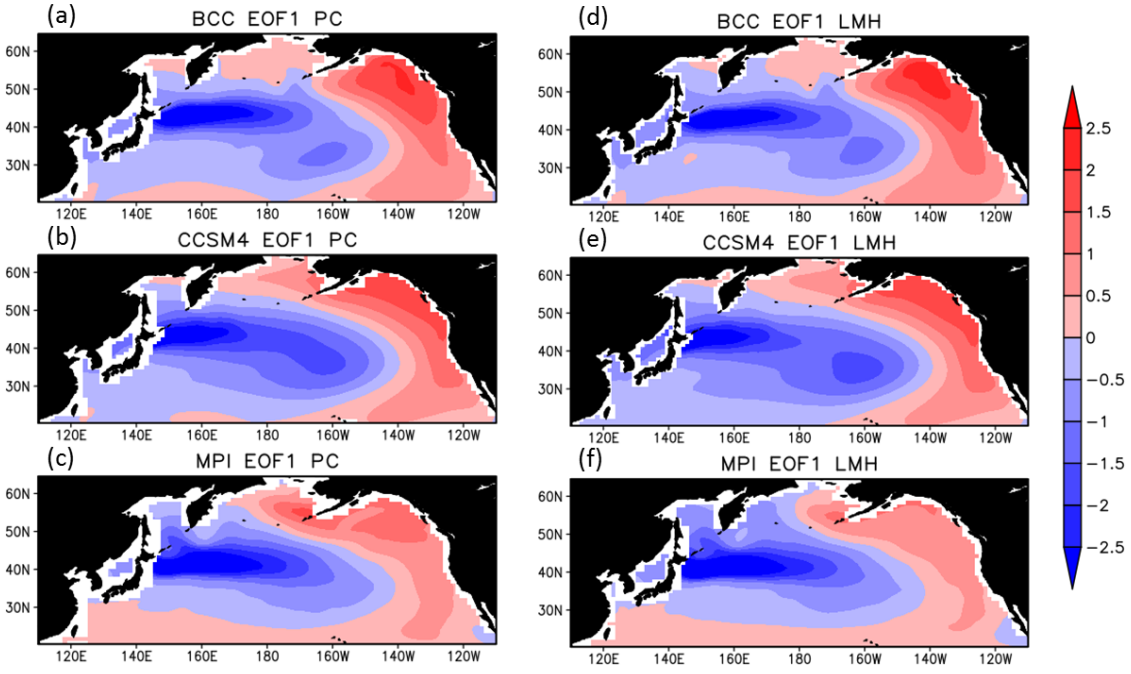

Figure 2: The PDO spatial pattern. The leading EOF of North Pacific SST anomalies for the three CMIP models, PC (a, b, c) and LMH (d, e, f) simulations.

Clim. Past Discuss., https://doi.org/10.5194/cp-2018-164
Manuscript under review for journal Clim. Past
Discussion started: 10 December 2018

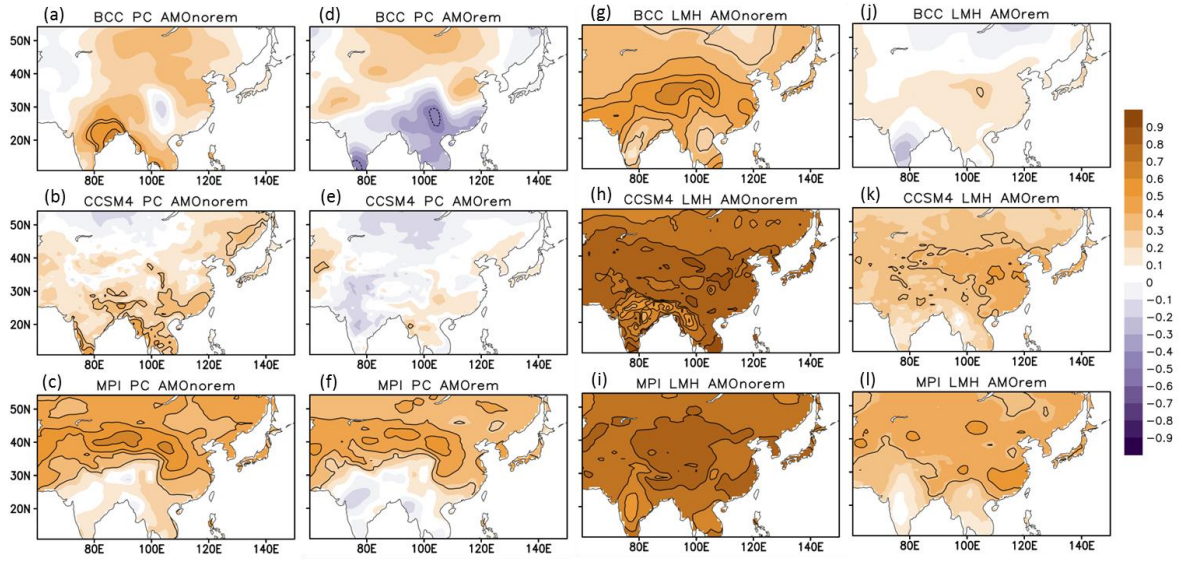

Figure 3: The correlation between AMO and East Asian surface temperature at multidecadal timescales for the three CMIP models for the PC (a, b, c and d, e, f) and LMH (g, h, i and j, k, l) simulations. Correlations using the AMO index with (AMOrem, d, e, f and j, k, l) and without (AMOnorem, a, b, c and g, h, i) subtracting global SST anomaly are also compared. The correlation values significant at 90% levels using two-tailed Student's t-test are contoured.

Clim. Past Discuss., https://doi.org/10.5194/cp-2018-164
Manuscript under review for journal Clim. Past
Discussion started: 10 December 2018

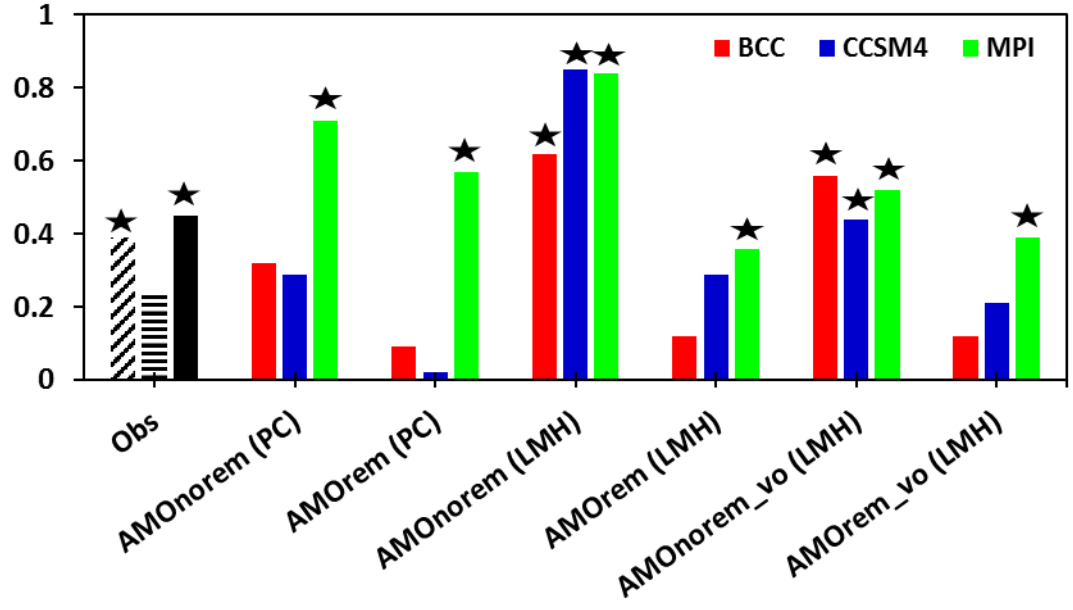

Figure 4: Correlations of E Asian regional average temperature against AMO for models and also for the reconstructions (30-year low pass filtered).The black dashed upward, dashed horizontal and solid bar are for observed correlation against TAS for WN17V, WN17O and AMN09 respectively. The groups of coloured bars are for different simulations (PC or LMH), different AMO definitions (global SST removed or not removed), and where the volcanic influence on E Asian temperature has been removed by linear regression (vo). The bars marked with 'star' marks are significance at 95% using a two-tailed student t-test. The correlation for reconstructed WN17O is weak (0.24) because it represents only internal AMO variability.

Clim. Past Discuss., https://doi.org/10.5194/cp-2018-164
Manuscript under review for journal Clim. Past
Discussion started: 10 December 2018

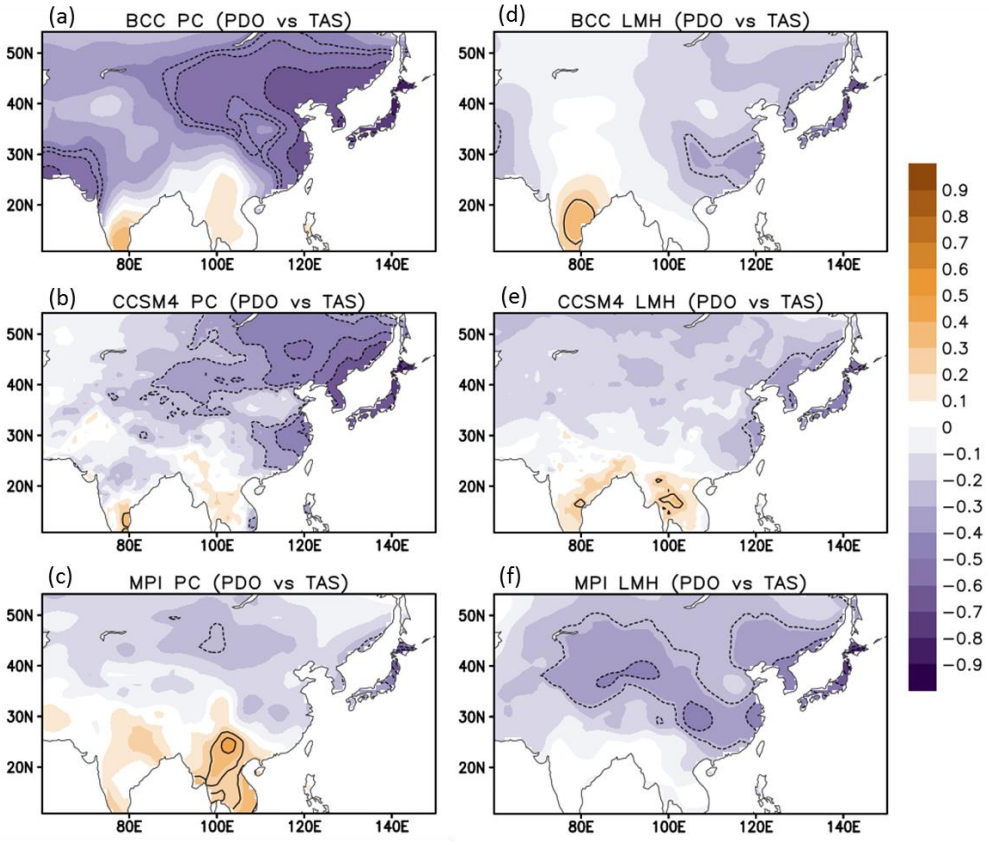

Figure 5: The correlation between PDO and East Asian surface temperature at multidecadal timescales for the three CMIP models for the PC (a, b, c) and LMH (d, e, f) experiments. The correlation values significant at 90% levels using two-tailed Student's t-test are contoured.

Clim. Past Discuss., https://doi.org/10.5194/cp-2018-164
Manuscript under review for journal Clim. Past
Discussion started: 10 December 2018

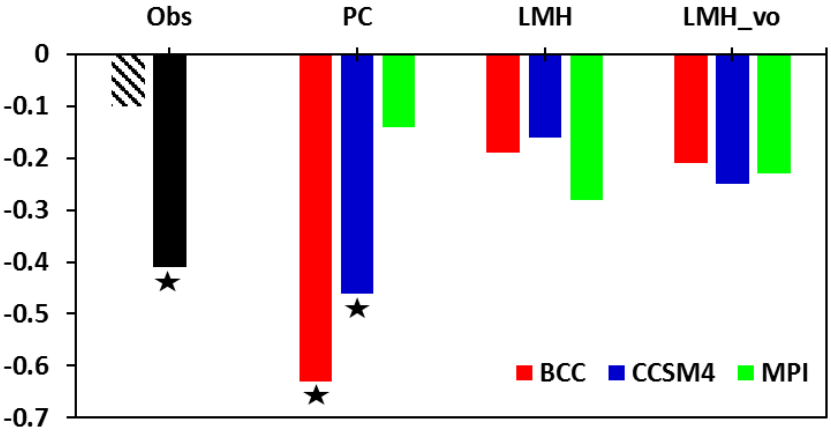

Figure 6: Correlations of E Asian regional average temperature against PDO for models and also for the reconstructions (30-year low pass filtered). The black dashed and solid bar are for observed correlation against TAS for MD05 and PMN09 respectively. The bars marked with 'star' marks are significance at 95% using a two-tailed student t-test.

Clim. Past Discuss., https://doi.org/10.5194/cp-2018-164
Manuscript under review for journal Clim. Past
Discussion started: 10 December 2018

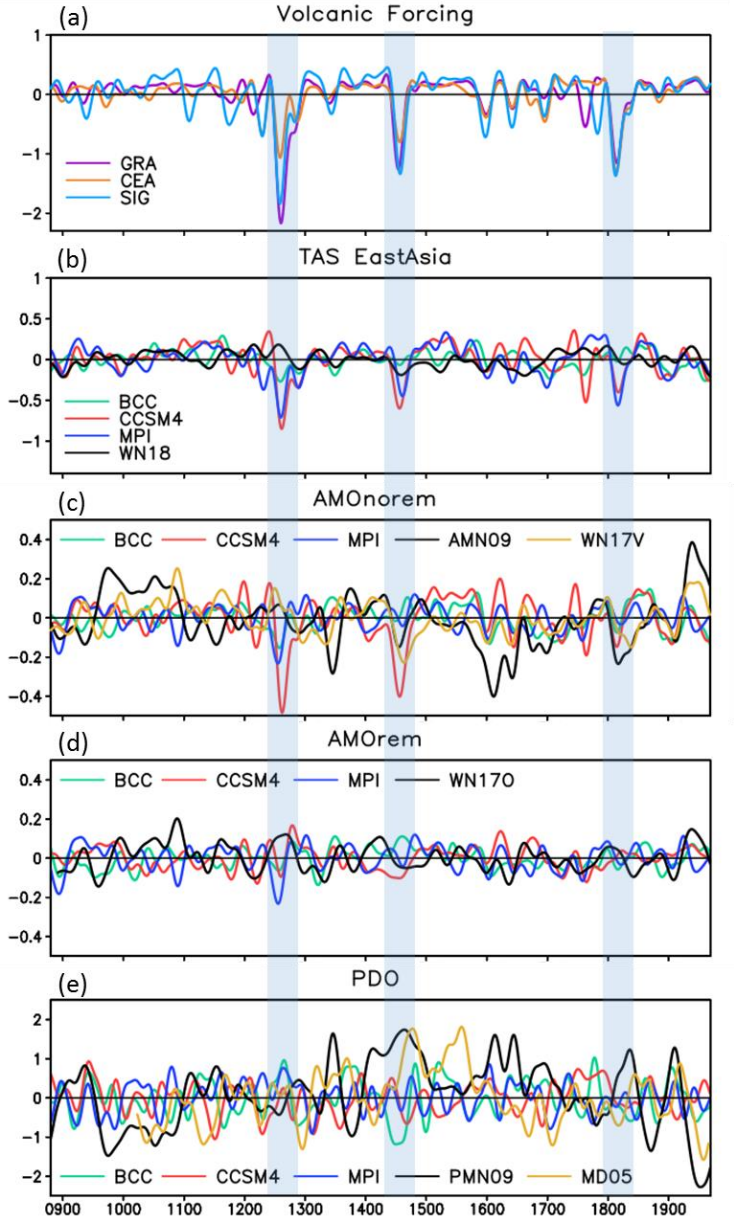

Figure 7: Timeseries of (a) volcanic forcing, (b) surface temperature over East Asia, (c) AMO index without subtracting the global SST, (d) AMO index after subtracting the global SST, and (e) PDO index, all passed through a 30-year low pass filter and truncated to remove filter end effects. Model simulation results are also compared with the available reconstructed data. MD05 PDO reconstructed data begins in 993, shorter than the other records. Blue vertical shading highlights the times when maxima of the filtered volcanic forcing occur.

Clim. Past Discuss., https://doi.org/10.5194/cp-2018-164
Manuscript under review for journal Clim. Past
Discussion started: 10 December 2018

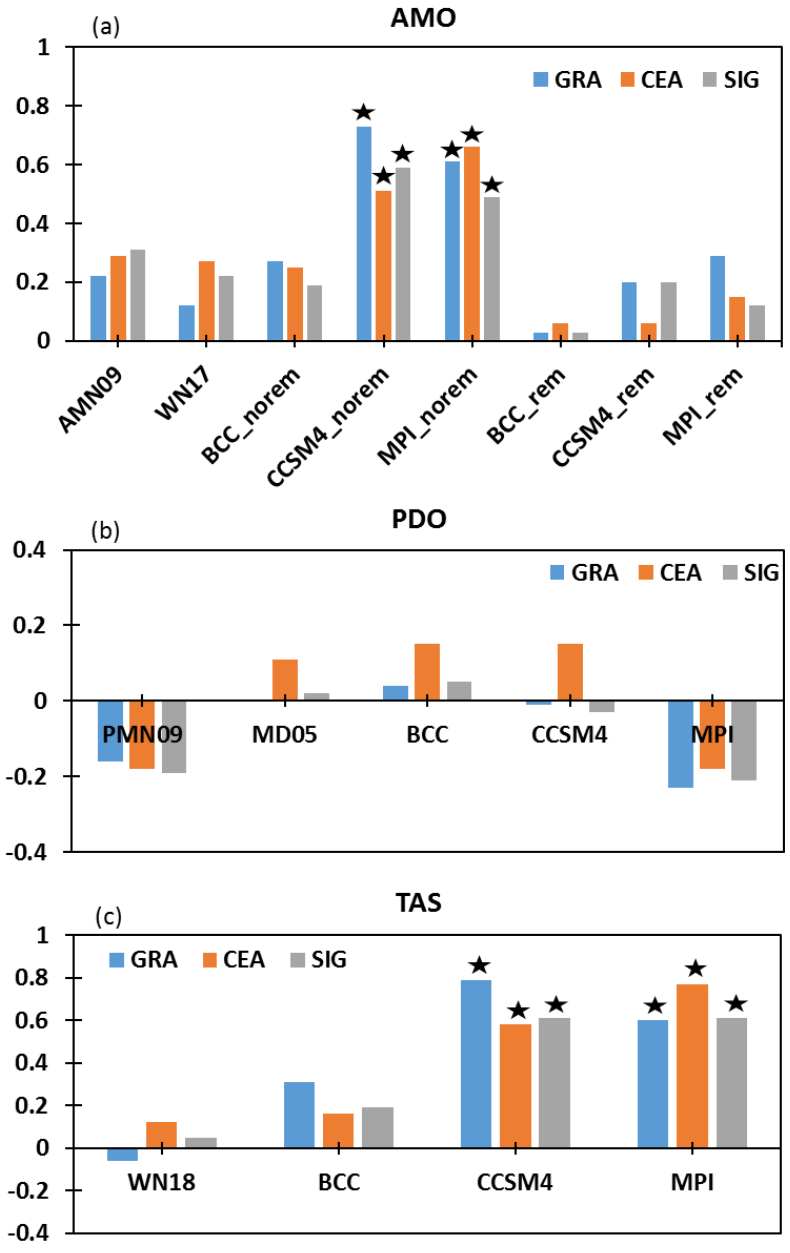

Figure 8: The correlations of (a) AMO, (b) PDO and (c) TAS with volcanic forcing (models and reconstructions)

Clim. Past Discuss., https://doi.org/10.5194/cp-2018-164
Manuscript under review for journal Clim. Past
Discussion started: 10 December 2018

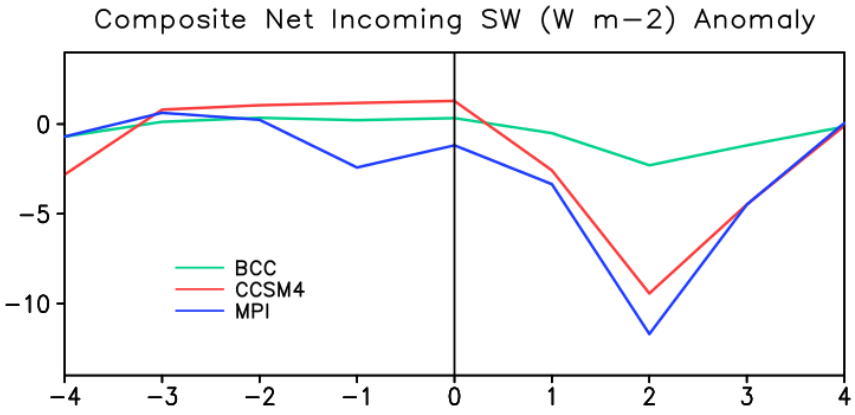

Figure 9: Annual mean composite anomaly of net shortwave radiation at the top of the atmosphere for three large volcanic eruption events (1257, 1458 and 1815). The zero vertical line is the year volcanic eruptions occurred and the numbers left and right of it are the years before and after the event.

Clim. Past Discuss., https://doi.org/10.5194/cp-2018-164
Manuscript under review for journal Clim. Past
Discussion started: 10 December 2018

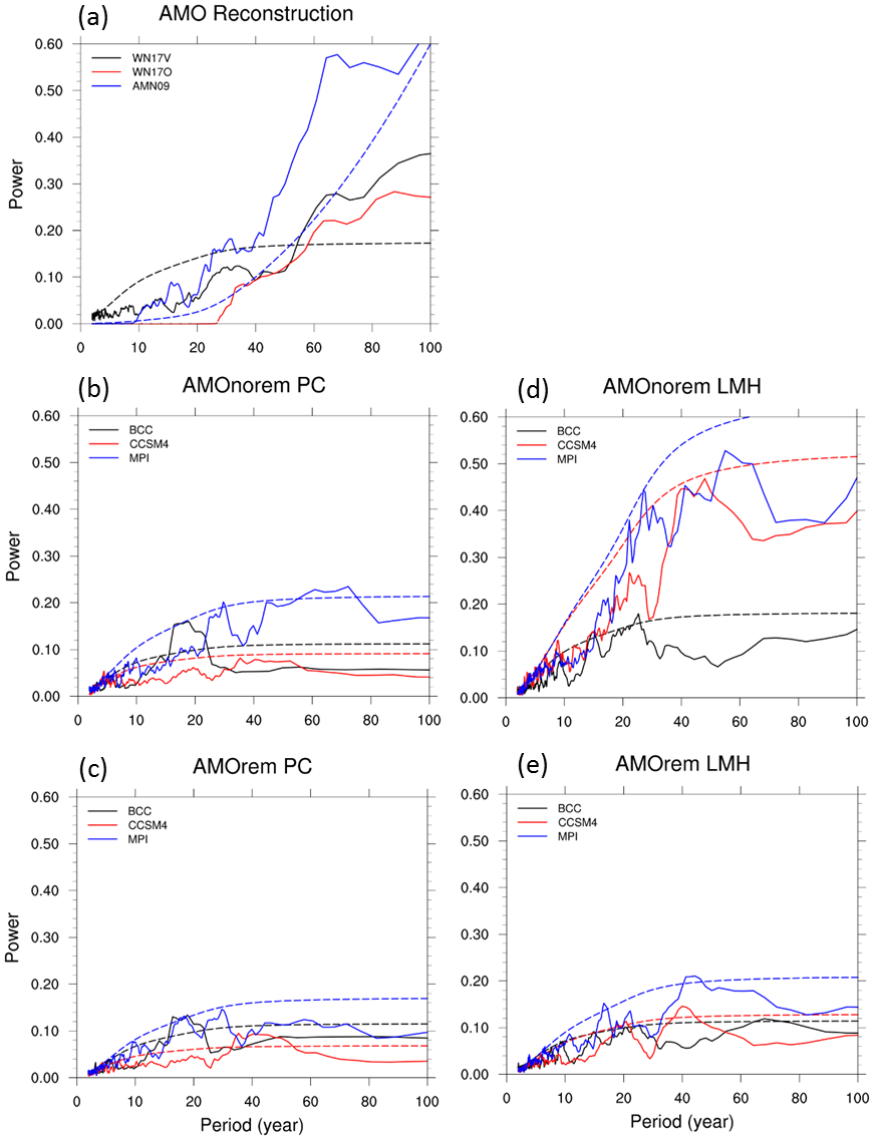

Figure 10 Spectra of AMO index of reconstructions (a) and three models for PC (b and c) and LMH (d and e) experiments and also AMO index with (c and e) and without (b and d) first subtracting the global SST anomaly. The solid lines are spectra and dashed lines are confidence at 90% level of periods with significantly higher variability than expected from an autoregressive spectrum. For WN17O (solid red line), the power for periods < 30 years is zero and should be ignored because only 30-year low-pass filtered data were available and hence the dashed line for confidence level is not presented (a).

Clim. Past Discuss., https://doi.org/10.5194/cp-2018-164
Manuscript under review for journal Clim. Past
Discussion started: 10 December 2018

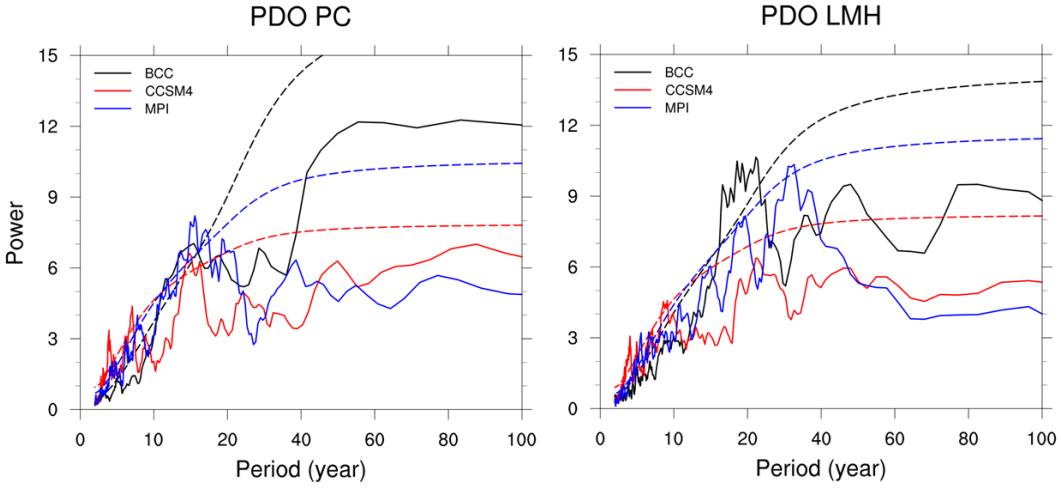

Figure 11: Spectra of PDO index of three models for PC and LMH experiments. The solid lines are spectra and dashed lines are confidence at 90% level of periods with significantly higher variability than expected from an autoregressive spectrum.